Copy Number Variations and Primary Open-Angle Glaucoma

Lea K. Davis,[1,2] *Kacie J. Meyer,*[2,3] *Emily I. Schindler,*[3] *John S. Beck,*[4] *Danielle S. Rudd,*[3] *A. Jason Grundstad,*[5] *Todd E. Scheetz,*[5,6] *Terry A. Braun,*[5,6] *John H. Fingert,*[3,6] *Wallace L. M. Alward,*[6] *Young H. Kwon,*[6] *James C. Folk,*[6] *Stephen R. Russell,*[6] *Thomas H. Wassink,*[3,7] *Val C. Sheffield,*[3,4,8] *and Edwin M. Stone*[3,6,8]

Purpose. This study sought to investigate the role of rare copy number variation (CNV) in age-related disorders of blindness, with a focus on primary open-angle glaucoma (POAG). Data are reported from a whole-genome copy number screen in a large cohort of 400 individuals with POAG and 500 age-matched glaucoma-free subjects.

Methods. DNA samples from patients and controls were tested for CNVs using a combination of two microarray platforms. The signal intensity data generated from these arrays were then analyzed with multiple CNV detection programs including CNAG version 2.0, PennCNV, and dChip.

Results. A total of 11 validated CNVs were identified as recurrent in the POAG set and absent in the age-matched control set. This set included CNVs on 5q23.1 (*DMXL1*, *DTWD2*), 20p12 (*PAK7*), 12q14 (*C12orf56*, *XPOT*, *TBK1*, and *RASSF3*), 12p13.33 (*TULP3*), and 10q34.21 (*PAX2*), among others. The CNVs presented here are exceedingly rare and are not found in the Database of Genomic Variants. Moreover, expression data from ocular tissue support the role of these CNV-implicated genes in vision-related processes. In addition, CNV locations of *DMXL1* and *PAK7* overlap previously identified linkage signals for glaucoma on 5p23.1 and 20p12, respectively.

Conclusions. The data are consistent with the hypothesis that rare CNV plays a role in the development of POAG. (*Invest Ophthalmol Vis Sci.* 2011;52:7122–7133) DOI:10.1167/iovs.10-5606

Glaucoma is a group of diseases characterized by progressive excavation of the optic disc caused by loss of the retinal ganglion cell axons. It causes peripheral visual field loss and if untreated can lead to blindness; it is the second leading cause of legal blindness in the United States. Primary open-angle glaucoma (POAG), the most common form in Western populations, is insidious in onset and affects 1% to 2% of the population over age 40. When POAG is observed in individuals under the age of 40 it is called juvenile open-angle glaucoma (JOAG). Increased intraocular pressure is a well-documented risk factor, but not a diagnostic criterion, for POAG.[1] More recently, reduced central corneal thickness (CCT) has been recognized as an important risk factor for glaucoma.[2] Medical and surgical treatments aimed at reducing intraocular pressure may be effective in preventing progressive visual loss in POAG patients, but treatment is often not implemented until significant, unrecoverable vision loss has occurred due to a lack of symptoms in early disease and delayed diagnosis (see Ref. 3 for a review).

Heritability estimates range from 0.36 to 0.57 for features of glaucoma, such as intraocular pressure and optic disc diameter, supporting the assertion that POAG has a strong genetic component.[4] Linkage analysis studies in large families segregating POAG in Mendelian fashion have identified 14 loci for the disease[5–23] (Table 1). Two causative genes have been identified through fine mapping of such linkage regions including myocilin (*MYOC*) at 1q23-q24[5,6] and optineurin (*OPTN*) at 10p13.[11] Together, variants in these genes are estimated to account for approximately 5% of POAG in the population at large.[11,24]

In this study, we investigated copy number variants (CNVs) as potential glaucoma-causing variation in individuals with POAG ascertained at the University of Iowa. CNVs are operationally defined as genomic insertions or deletions that are larger than 1 kb and not a result of transposable elements. CNVs often escape detection in traditional studies of genetic variation, such as direct sequencing, single-strand conformation polymorphism analysis, and single-nucleotide polymorphism (SNP) association studies. CNVs are now recognized as a major contributor to human genetic variation and have been associated with other genetically complex disorders including autism, schizophrenia, HIV/AIDS susceptibility, and Crohn's disease.[25–34]

The eye is a highly specialized organ that has shown significant sensitivity to dosage changes of key developmental and regulatory genes, making glaucoma an excellent phenotype for

From the [1]Department of Psychiatry, University of Illinois, Chicago, Illinois; and the [3]Interdisciplinary Genetics Program, the Departments of [4]Pediatrics, [6]Ophthalmology and Visual Sciences, and [7]Psychiatry, the [5]Center for Bioinformatics and Computational Biology, and the [8]Howard Hughes Medical Institute, University of Iowa, Iowa City, Iowa.

[2]These authors contributed equally to the work presented here and should therefore be regarded as equivalent authors.

Supported by Alcon Research, Ltd. (Fort Worth, TX), which provided funds for the purchase of the SNP genotyping chips; National Institutes of Health Predoctoral Training Grant T32GM008629 (LKD); National Institutes of Health Grants R01-EY-010564 (VCS) and R01-EY-016822 (EMS); the Carver Endowment for Molecular Ophthalmology (EMS, VCS); Research to Prevent Blindness (Department of Ophthalmology, University of Iowa), Career Development Awards (TES, JHF), and the Lew Wasserman Award (WLMA); and the Foundation Fighting Blindness. VCS and EMS are investigators at the Howard Hughes Medical Institute.

Submitted for publication March 31, 2010; revised August 6 and October 3, 2010; accepted November 1, 2010.

Disclosure: **L.K. Davis**, None; **K.J. Meyer**, None; **E.I. Schindler**, None; **J.S. Beck**, None; **D.S. Rudd**, None; **A.J. Grundstad**, None; **T.E. Scheetz**, None; **T.A. Braun**, None; **J.H. Fingert**, None; **W.L.M. Alward**, None; **Y. Kwon**, None; **J.C. Folk**, None; **S.R. Russell**, None; **T.H. Wassink**, None; **V.C. Sheffield**, None; **E.M. Stone**, None

Corresponding author: Val C. Sheffield, 4181 Medical Education Research Facility, University of Iowa, 375 Newton Road, Iowa City, IA 52242; val-sheffield@uiowa.edu.

TABLE 1. Known Glaucoma Loci Identified through Linkage Analysis

Glaucoma Linkage Loci	Chromosomal Position	OMIM Number	Reference
GLC1A	1q22	137750	Sheffield et al.[5]
GLC1B	2cen-q13	606689	Stoilova et al.[7]
GLC1C	3q21-q24	601682	Wirtz et al.[8]; Kitsos et al.[9]
GLC1D	8q23	602429	Trifan et al.[10]
GLC1E	10p	602432	Rezaie et al.[11,12]
GLC1F	7q35-q36	603383	Wirtz et al.[13]
GLC1G	5q21.3-q13	609669	Monemi et al.[14]
GLC1H	2p16-p15	611276	Suriyapperuma et al.[15]
GLC1I	15q11-q13	609745	Wiggs et al.[16]; Allingham et al.[17]
GLC1J	9q22	608695	Wiggs et al.[18]
GLC1K	20p12	608696	Wiggs et al.[18]
GLC1L	3p21–22	137750	Baird et al.[20]
GLC1M	5q22.1-q32	610535	Pang et al.[21]; Fan et al.[22]
GLC1N	15q22–24	611274	Wang et al.[23]

Linkage locus name is given along with cytoband position, OMIM identification number, and discovery reference.

CNV screening. Select copy number mutations have been known to play a role in glaucoma and related disorders of vision for some time, including deletions of *LMXB1*, *FOXC1*, and 4q34, among others.[35–37] Gross karyotypic abnormalities of 9p23 and trisomies of chromosome 13 have been associated with developmental glaucoma.[38–40] Recent fine mapping of 6p25, the *FOXC1* locus, has provided evidence of a spectrum of mechanisms by which deletions and duplications of the *FOXC1* gene occur.[37,41,42] The initial clue that *FOXC1* is involved in glaucoma was based on a chromosomal abnormality found in a single patient, demonstrating the value of identifying rare variants that may identify candidate genes and loci for disease causation.

One recent study of 27 glaucoma patients and 12 controls analyzed by array comparative genome hybridization (CGH) methods found no CNVs in either patients or controls.[43] However, the ability to detect disease-associated CNVs in this sample was limited due to (1) array CGH probe density (2) small sample size, and (3) single algorithm copy number calls. Before the present study, there have been no large-scale studies of copy number variation (CNV) in glaucoma. The development of software to analyze signal intensity data from high-density SNP-based array platforms, coupled with confirmation by quantitative PCR, enabled us to undertake a detailed cataloguing of CNVs in 400 POAG patients and 500 control subjects.

METHODS

Patient Diagnosis and Ascertainment

This study was conducted with the approval of the Institutional Review Board of the University of Iowa and in compliance with the Declaration of Helsinki. Four hundred unrelated individuals with the clinical diagnosis of POAG and 500 individuals with no signs of glaucoma were enrolled in the study after providing informed consent. The cohort of glaucoma subjects underwent a complete battery of ophthalmic tests, including a dilated stereoscopic examination of the optic nerve heads, Goldmann applanation tonometry, gonioscopy, optic nerve head photography, perimetry, and slit lamp examination. Visual fields were assessed with standard automated perimetry (SAP; the SITA 24-2 program on the Humphrey Field Analyzer; Carl Zeiss Meditec, Dublin, CA). Patients unable to perform automated perimetry were tested with Goldmann manual kinetic perimetry (Haag-Streit Instruments, Köniz, Switzerland).

Patients exhibiting optic nerve head excavation and associated glaucomatous visual field loss in at least one eye were considered to have glaucoma. Glaucomatous optic nerves were defined as nerves with cup-to-disc ratios of greater than 0.7, thinning of the neural rim, asymmetry of the optic nerve cup-to-disc ratio of >0.2, or photographic documentation of progressive loss of the neural rim. Patients were required to have visual fields of adequate quality for interpretation. For visual field perimetry adequate quality required a false-positive rate, false-negative rate, and fixation loss rate of less than 33%.[44] SAP visual field evidence of glaucoma was based on the Collaborative Normal Tension Glaucoma Treatment Trial criteria.[45] Patients screened using manual kinetic perimetry were required to exhibit depression of the visual field in an arcuate pattern with respect to the nasal horizontal meridian. Patients were enrolled without regard to IOP. Seventy-four of the 400 subjects had never been reported to have IOP over 21 mm Hg and could be categorized as having normal-tension glaucoma.

Age-matched contrast and control subjects were enrolled from the same patient population at the University of Iowa and were judged to have no signs of glaucoma after a complete eye examination by a board-certified ophthalmologist and/or review of eye clinic charts. Because of the many challenges associated with recruitment of older individuals free of any eye phenotype, we included in our study 400 contrast macular degeneration patients under observation in the Retina Clinic and 100 normal control subjects with neither POAG nor macular degeneration who were attending the Comprehensive Ophthalmology Clinic. All contrast and control patients were rigorously evaluated for any signs or symptoms of glaucoma, to ensure that they could serve as a glaucoma-free cohort. Symptoms consistent with a diagnosis of glaucoma were considered grounds for exclusion of any control or contrast patients. Additional exclusion criteria included a family history of glaucoma, age at enrollment of less than 59 years, and any history of medication used to treat elevated intraocular pressure.

Experimental Design

Experimental design and workflow is shown in Figure 1. This study was designed to identify rare and recurrent CNVs that increase risk for development of glaucoma. A total of 400 patients with glaucoma and 500 glaucoma-free age-matched controls were analyzed with SNP microarrays (GeneChip; Affymetrix, Santa Clara, CA). Two hundred glaucoma patients and 200 controls were analyzed with the 500K two-chip SNP array. The remaining 200 glaucoma patients and 300 nonglaucoma controls were analyzed with the more recently released 5.0 SNP arrays. All data were analyzed with two CNV detection programs. All arrays were analyzed with PennCNV.[46] In addition, all 500K SNP arrays were analyzed with Copy Number Analyzer for GeneChip (CNAG),[47] and all 5.0 SNP arrays were analyzed with dChip.[48,49] After both array-based and variant-based quality control measures were implemented, a total of 11,680 CNVs were called (Supplementary Table S1, http://www.iovs.org/lookup/suppl/doi:10.1167/iovs.10-5606/-/DCSupplemental). This complete data set was termed the single criterion set, as it included all CNVs

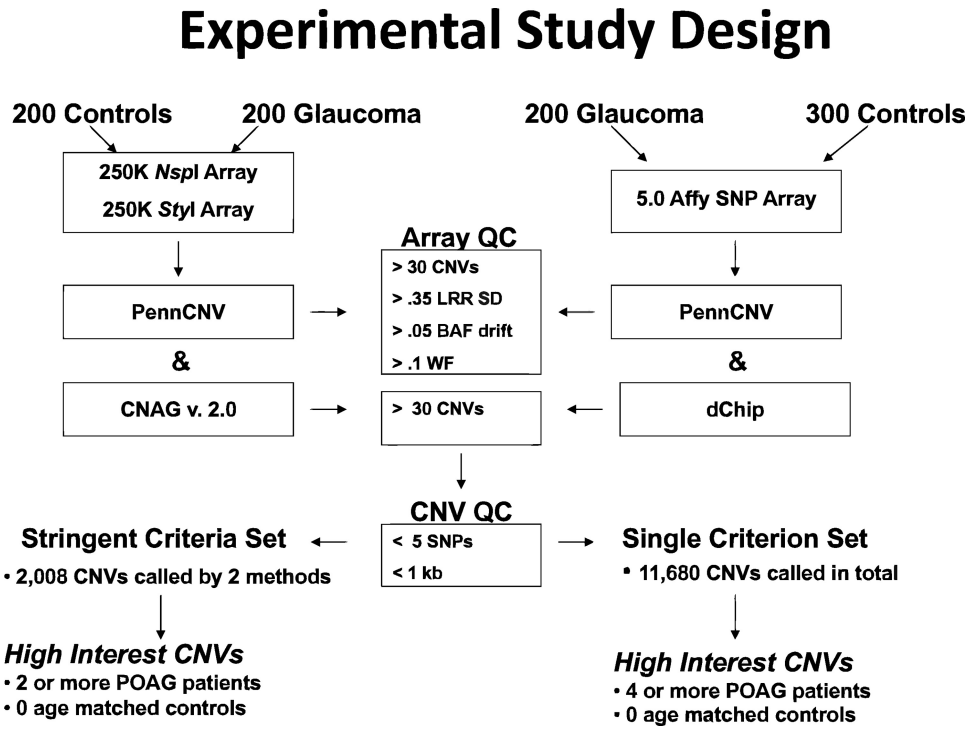

FIGURE 1. Experimental design workflow. A total of 400 patients with glaucoma and 500 controls were run on high-density genotyping arrays. Two hundred individuals with glaucoma and 200 controls were run on the 500K mapping array set. Another 200 glaucoma patients and 300 controls were run on the 5.0 SNP array. Both sets of arrays were analyzed with two programs. The *Nsp*I and *Sty*I arrays were analyzed separately with PennCNV and CNAG. The 5.0 arrays were analyzed with PennCNV and dChip. Array-based and CNV-based quality control metrics were applied to result in a total data set of 11,680 CNVs called by any program on any array (single criterion set). We then examined this data set for CNVs that were called by two programs or were present on two platforms, resulting in 2008 CNVs (stringent criteria set). High interest CNVs were then indentified by comparing POAG patients to controls and identifying CNVs present exclusively in the glaucoma cohort.

called with any single program. From the single criterion set, we developed a second set of 2008 high-confidence CNVs that were called by multiple algorithms. We termed these the stringent criteria set.

CNVs were considered to be of interest with respect to glaucoma causation if they met one of the following criteria: (1) They were from the stringent criteria set and were present at least twice in the glaucoma patient group while absent from the controls. (2) They were from the single criterion set and present in at least four glaucoma cases while absent from controls. It should be noted that single-call CNVs found in a control were validated by quantitative (q)PCR in that control sample. If the CNV was confirmed, it was used as an additional filtering criterion to remove the CNV under question from the high-interest group. All CNVs in the potential risk set were validated by qPCR or array-based comparative genomic hybridization (a-CGH).

Human-Mapping 250K Microarray

DNA from each individual was analyzed with the 500K Affymetrix microarray (*Nsp*I and *Sty*I). The DNA was hybridized to the array according to the manufacturer's instructions. Briefly, the assay uses 250 ng of genomic DNA digested with *Nsp*I and *Sty*I (New England Biolabs, Boston, MA), ligated to an adaptor using T4 DNA ligase (New England Biolabs), and amplified by PCR using *Taq* (Titanium; Clontech, Palo Alto, CA). PCR products were then purified from excess primer and salts by a DNA amplification cleanup kit (Clontech), and a 90-μg aliquot was fragmented using DNase I. An aliquot of the fragmented DNA was separated and visualized in a 3% agarose gel in 1× TBE buffer, to ensure that the bulk of the product had been properly fragmented. The fragmented samples were end-labeled with biotin using terminal deoxynucleotidyl transferase before each sample was hybridized to the array for 16 hours at 49°C. After hybridization, the arrays were washed and stained (Fluidics Station 450; Affymetrix). The most stringent wash was 0.6× SSPE, 0.01% Tween-20 at 45°C, and the samples were stained with *R*-phycoerythrin (Invitrogen-Molecular Probes, Eugene, OR). Imaging of the microarrays was performed with a high-resolution scanner (GCS3000; Affymetrix).

Genome-Wide Human SNP *Nsp/Sty* 5.0 Microarray

DNA from an additional 200 patients with diagnosed AMD and 300 age-matched controls was prepared and hybridized to a genome-wide human SNP *Nsp/Sty* 5.0 Microarray according to the manufacturer's instructions (Affymetrix). The 5.0 array interrogates same SNPs contained on the human mapping 500K array set (GeneChip; Affymetrix) and contains additional nonpolymorphic probes used for copy number detection. Genomic DNA was digested with either *Nsp*I or *Sty*I and ligated to adaptors that allow PCR amplification of DNA fragments ranging in size from 200 to 1,100 bp. *Nsp*I and *Sty*I PCR products were then pooled and purified before fragmentation. Fully fragmented samples were labeled with biotin and hybridized to the array at the University of Iowa DNA Facility. Arrays were washed and stained (Fluidics Station 450; Affymetrix) and then scanned (GCS3000 high-resolution scanner; Affymetrix).

CNV Detection

Three publicly available programs (PennCNV, dChip, and CNAG) were used to detect copy number changes. After analyzing the arrays, we

developed quality control metrics that were based on their performance.

PennCNV Analysis

A total of 1300 arrays were analyzed with PennCNV.[46] Five hundred 5.0 arrays, 400 250K *Sty*I arrays, and 400 250K *Nsp*I arrays (*Nsp*I and *Sty*I arrays were run on the same cohort) were run on individuals, some with and some without glaucoma. On advice provided by the developer of PennCNV, Kai Wang at the University of Pennsylvania, we developed quality control metrics empirically using the present data set. We adjusted the acceptable logR ratio to 0.35, and the B-allele frequency (BAF) drift and wave factor (WF) thresholds were set at 0.05 and 0.1, respectively. The logR ratio is a measure of total fluorescent signal intensity measured at every probe on a log-normalized scale of −1 to 1 and is proportional to the copy number at that locus. As noise is inherent in these data, we determined an empiric standard deviation threshold of 0.35 and regarded any array with a logR SD above 0.35 as containing unacceptable background noise for reliable CNV detection. BAF drift is a measure of allelic specific signal intensity and samples exceeding a drift value of 0.05, displayed an excessive number of duplications. The WF metric refers to variation in the hybridization intensity and causes waviness in the logR signal patterns from the arrays.[33] The WF metric is a function of GC content; probe location, and starting DNA quantity. WF thresholds were set at 0.1 to eliminate arrays with unacceptable wave patterns in the signal intensity data. In addition, we removed any arrays with more than 30 CNV calls as part of the array-based quality control. From this body of CNVs we then removed any individual CNV that was called by fewer than five SNPs or was less than 1 kb in size as part of the CNV-based quality control. The remaining data represents the 90th performance percentile and above. The data were analyzed for copy number using a hidden Markov model (HMM) which identifies patterns in the signal intensity data and infers the true "hidden" copy number state that generated such a pattern.

CNAG Analysis

CNAG was used to analyze all 400 *Sty* and 400 *Nsp* arrays run on glaucoma patients and controls.[47] Quality control measures for CNAG were developed to be more inclusive and rely heavily on the stringency of CNV detection by the program. Instead of comparing each array to all other arrays, CNAG uses 5 to 10 best fit reference arrays drawn from the entire set of *Sty*I and *Nsp*I arrays based on similarity of signal intensity standard deviation values. CNAG also applies an HMM to the data, highlighting chromosomal regions with significant deviation in signal intensity. CNVs were then manually detected and annotated from the CNAG graphic output. Arrays with high logR ratio standard deviations resulting in fewer than five appropriate references were not included in the final analysis. Arrays with more than 30 copy number variants were removed, and CNVs less than 1 kb in size or called by fewer than five SNPs were also excluded.

dChip Analysis

Five hundred 5.0 arrays run on individuals with and those without glaucoma were also analyzed with dChip.[48,49] The arrays were analyzed in batches of 50. For each array, the remaining 49 arrays within the batch were used as the reference sample. Signal intensity data from each raw data array file was normalized using the "invariant set normalization" method which identifies a subset of probes with small rank difference in signal intensity across the arrays that then becomes the "invariant set" or the basis for development of a normalization curve. Once signal intensity was adjusted across arrays, model-based expression indexes (MBEIs) were determined using the "perfect match only" model to reduce background signals, identify outlier probes, and calculate corrected SNP intensity values.[50] As there is no strictly "normal" sample where a ploidy of 2 is known to exist throughout the genome, a 10% trimmed analysis was used. This method assumes that for any given SNP, less than 10% of the samples tested will show deviation in copy number. Thus for each SNP, 5% of samples with extreme signal values from each end are removed as outliers, and the remaining samples are used to estimate corrected signal intensity values and standard deviations based on a ploidy of 2 at that SNP position. This method may result in undercalling common CNVs that are present in greater than 10% of the sample, but by increasing the trimmed analysis, one also runs the risk of undercalling rare CNVs. To detect changes in copy number, an HMM was applied to the signal intensity data with a maximum moving window of 1000 SNPs. Arrays with more than 30 copy number variants were removed, and CNVs less than 1 kb in size or called by fewer than five SNPs or were also excluded.

CNV Validation

Quantitative Real-Time PCR. For qPCR, we designed three primer sets within the center of the CNV to be validated. We used an assay targeted for *G6PD* on the X chromosome as an internal control for gene dosage and an assay targeted for *GAPDH*, to normalize the signal between replicate DNA samples. As the possibility for CNV exists for any given region of the genome, we relied on information obtained from our arrays as well as our sex prediction within the qPCR experiment to support the use of *GAPDH* as a normalization control for validation of copy number variants. In addition, we used a pooled reference sample as our calibrator (Male or Female Genomic DNA; Promega, Madison, WI) to ensure the calibrator sample had a ploidy of 2 at all genomic loci. For each CNV that required validation, we began with a single qPCR assay. If that initial assay was in agreement with the CNV call from the array analysis, we regarded the result as confirmation. If the first qPCR assay was in conflict with the results from the array, we used the second qPCR assay to reconfirm. The third qPCR assay was used if results from either the first or second qPCR assay were inconclusive. In a small number of cases, qPCR methods were unable to validate or invalidate the CNV being tested. In these cases, array-based comparative genomic hybridization (aCGH) methods were used to confirm CNVs.

The qPCR reactions were performed in mixtures containing 12.5 μL of 2× SYBR green PCR master mix (QuantiTect; Qiagen, Valencia, CA), 12 μL genomic DNA (1ng/μL), 0.25 μL of each primer (10 picomoles/μL) in a total volume of 25 μL The PCR amplification and detections were performed on a PCR system (model 7500; Applied Biosystems, Inc., [ABI], Foster City, CA) each with an initial activation step for 15 minutes at 95°C followed by 15 seconds at 94°C, 30 seconds at 55°C, and 30 seconds at 72°C for 42 cycles. The threshold cycle value was calculated using the $^{\Delta\Delta}C_T$ method. C_T was determined using the thermocycler software, and an average of three replicates was calculated. The fold change from the calibrator sample (Male or Female Genomic DNA; Promega) at 1 and the ratio of the normalized fold change in the test sample compared to that of the calibrator sample was calculated.

Array-based Comparative Genomic Hybridization (aCGH). One microgram of patient DNA and 1 μg of reference DNA (Promega) were fluorescently labeled in parallel followed by co-hybridization to a 385K chromosome-specific tiling array (Nimblegen; Roche, Indianapolis, IN). The array was scanned (4000B GenePix; Molecular Devices, Sunnyvale, CA) and signal intensity data were analyzed using an algorithm within the accompanying software (segMNT, Nimblegen; Roche). A browsing interface for the arrays (SignalMap software; Roche) was used to visualize the array CGH data as a graphic output.

Results

Two different arrays, each analyzed by two independent programs, were used in this study. Use of different arrays and programs provided us an opportunity for array performance comparisons. All CNVs detected by all programs in all patients and controls are provided in the supplementary materials (Supplementary Table S1, http://www.iovs.org/lookup/suppl/doi:10.1167/iovs.10-5606/-/DCSupplemental). In addition, all CNVs identified in individuals with high interest CNVs are provided in

Table 2. Descriptive Statistics for CNVs Identified in the POAG Cohort

	Two Chip Mapping 500K Array Set (CNAG and PennCNV)	SNP 5.0 Array (dChip and PennCNV)
Arrays, *n* (QC Pass)	400 (376)	200 (194)
Deletions, average across analysis programs	657	870
Duplications, average across analysis programs	526	595
Average number of CNVs per person	3.14	7.55
Average size of deletions (SD)	267,343 bp (409,790)	99,024 bp (226,711)
Average size of duplications (SD)	571,490 bp (611,411)	272,612 bp (380,289)

Data from the two programs used to analyze the arrays has been averaged to reflect array performance as opposed to program performance. The *Nsp*I and *Sty*I subarrays from the 500K mapping set were analyzed separately for CNV detection. Data from the two-chip mapping 500K array presented here represent an average between programs and between the *Nsp*I and *Sty*I chips. QC, quality control.

Supplementary Table S2 (http://www.iovs.org/lookup/suppl/doi:10.1167/iovs.10-5606/-/DCSupplemental).

Descriptive Data from the 500K SNP Microarray

The 500K two-chip arrays (*Nsp*I and *Sty*I analyzed separately) were analyzed with PennCNV and CNAG and detected an average of 3.14 CNVs per subject (Table 2). There were no significant differences in the average number of CNVs, the average number of deletions and duplications, or the average size of deletions and duplications between individuals with glaucoma and controls on the 500K two-chip platform (Tables 2, 3). More CNVs were detected on chromosomes 14, 15, and 16 than on the other chromosomes, regardless of the analysis method used, which is reflective of the CNV hotspots on these chromosomes, which can be detected with 250K arrays.

Descriptive Data from 5.0 Affymetrix SNP Microarray

We found that the 5.0 array platform detected an average of 7.55 CNVs per POAG patient (Table 2). There were no significant differences in the average number of CNVs per patient, the average number of deletions or duplications, or the average size of deletions or duplications between individuals with glaucoma and controls on the 5.0 SNP array (Tables 2, 3). There was a trend for increased calls on chromosomes 1, 14, 15, 16, 17, and 22. This trend again reflects regions of common CNV that can be detected with the SNP density present on the 5.0 array.

The 5.0 SNP array detected nearly twice as many CNVs per person than the 500K two-chip mapping array. This increase is due to increased SNP density and the presence of copy number probes on the 5.0 array. In addition, the average size of deletions and duplications detected with the 5.0 array was significantly smaller than those detected on the 500K two-chip array, due again to the increased density of SNPs on the 5.0 array.

Array CNV Validation

A total of 46 CNVs met criteria for validation by qPCR or aCGH. Thirty-one of these CNVs were only detected by a single program and 24 (77%) of 31 were validated as true calls. Two programs called the remaining 15 CNVs, and 14 of 15 were confirmed by either qPCR or aCGH (93%). A total of 11 CNVs remained after validating and applying the cross-referenced criteria (Table 4). This set included CNVs on 5q23.1 (*DMXL1*, *DTWD2*), 20p12 (*PAK7*), 12q14 (*C12orf56*, *XPOT*, *TBK1*, and *RASSF3*), and 12p13.33 (*TULP3*), among others. Validation data from qPCR and aCGH for the high-interest CNV set is included in Supplementary Table S3 and Supplementary Figures S1 and S2 (http://www.iovs.org/lookup/suppl/doi:10.1167/iovs.10-5606/-/DCSupplemental).

Discussion

The results of this large study indicate that rare CNVs do not account for a large proportion of cases of glaucoma. Although we did not find an increased overall genomic burden of CNVs in glaucoma, we did identify several specific genes implicated by rare and recurrent CNVs in glaucoma patients. The approach taken in this study was conservative, and it is possible that it underestimates the contribution of common CNVs as well as CNVs smaller than 1 kb. CNVs less than 1 kb

Table 3. Descriptive Statistics for CNVs Identified in the Controls

	Two Chip Mapping 500K Array Set (CNAG and PennCNV)	SNP 5.0 Array (dChip and PennCNV)
Arrays, *n* (QC Pass)	400 (373)	300 (294)
Deletions, average across analysis programs	682	1,120
Duplications, average across analysis programs	510	893
Average number of CNVs per person	3.19	6.80
Average size of deletions (SD)	257,007 bp (396,361)	111,586 bp (226,891)
Average size of duplications (SD)	536,297 bp (601,621)	259,616 bp (355,980)

Data from the two programs used to analyze the arrays has been averaged to reflect array performance as opposed to program performance. The *Nsp*I and *Sty*I sub-arrays from the 500K mapping set were analyzed separately for CNV detection. Data from the two-chip mapping 500K array presented here represent an average between programs and between the *Nsp*I and *Sty*I chips. QC, quality control.

TABLE 4. CNVs of High Interest

Gene Name	Cytoband	Approximate Size (kb)	Type	Individuals (*n*)	Novel to DGV	Validation Method	Gene Function
NT5C1B	2p24.2	144	Deletion	2	No	qPCR	Cytosolic 5′ nucleotidase
IMMT	2p11.2	217	Duplication	2	No	qPCR	Mitochondrial inner membrane protein
NPHP1	2q13	147	Duplication	2	No	qPCR	Control of cell division, cell–cell and cell-matrix adhesion
No RefSeq genes	5p15.33	60	Duplication	4	Yes	qPCR	N/A
DMXL1, DTWD2	5p23.1	776	Both	2	Yes	qPCR	*DMXL1*-WD domain containing; *DTWD2* - no known function
CD5, CD6	11q12.2	145	Duplication	2	Yes	qPCR	Glycoproteins involved in T-cell activation
C12orf56, TBK1, XPOT, RASSF3	12q14.2	486	Duplication	2	Yes	aCGH	*C12orf56,* hypothetical protein; *XPOT,* tRNA exportin *TBK1,* Mediates NFKB activation *RASSF3,* Ras association domain containing protein
TULP3	12p13.33	20	Deletion	5	Yes	qPCR	Retina expressed transcription factor
FAM27L	17p11.2	482	Duplication	4	No	qPCR	No known function
No RefSeq genes	18p11.32	89	Deletion	3	No	qPCR	N/A
PAK7	20p12	144	Duplication	2	Yes	aCHG	Brain-expressed kinase involved in neurite growth

Included are genes in CNV region, cytoband location, approximate size averaged across multiple programs and individuals, CNV type and the number of individuals with the given CNV, the presence or absence of the CNV in the database of genomic variants (Iafrate et al., 2004), method of validation (qPCR or aCGH), and the gene function. Exact breakpoints determined by each program in each individual are available in Supplementary Table S1 (http://www.iovs.org/lookup/suppl/doi:10.1167/iovs.10–5606-/DCSupplemental).

are difficult to reliably ascertain on most SNP array platforms and often have low validation rates. It is also important to note the challenges faced when differentiating benign CNVs from those associated with disease. Our results should be interpreted with a degree of caution, as these are rare events, and thus their observation in a few patients may be by chance. Nevertheless, they meet the rigorous criteria that we established and are presented with the caveat that additional evaluation is necessary to conclusively confirm or reject their role in glaucoma.

A total of 11 CNVs were identified as being of interest in the glaucoma cohort. Two of these CNVs highlight genes, *PAK7* and *DMXL1*, that lie within previously identified JOAG linkage intervals, and a third CNV encompasses *TBK1*, the binding partner of a known glaucoma gene, optineurin.

Duplication of 20p12 (*PAK7*)

Two overlapping but unique CNVs were detected on 20p12 within the previously reported 12.7-Mb glaucoma locus, GLC1K.[18,19] These CNVs result in duplication of the first two exons of p21 protein (Cdc42/Rac)-activated kinase 7 (*PAK7*; Fig. 2A). The duplications are novel to the Database of Genomic Variants (DGV) and were not identified in 862 additional controls analyzed with the 6.0 SNP array (Affymetrix) at the University of Toronto (Marshall C, personal communication, 2009). *PAK7*, also known as *PAK5*, is one of the group II Pak genes. *PAK7* is expressed in neural projections and is highly expressed in the human eye including the retina and ganglion cell layer (data from microarray expression studies of 10 ocular tissues conducted in collaboration with Alcon, Fort Worth, TX; data not shown).[51] It is an effector of an Rac/CDC GTPase and is thought to regulate cytoskeletal dynamics, proliferation, and apoptosis.[52]

The clinical findings in one of the two patients with a *PAK7* duplication (GGA-410-1) were remarkable for thin CCT (Table 5). Neither patient had a positive family history of glaucoma or were parents of these subjects available for study to determine whether the *PAK7* CNVs were inherited or arose de novo. The breakpoints of these CNVs, however, were different, and genotype analysis showed two distinct duplication haplotypes suggesting that they did not share an ancestral event. Our data, along with known expression profiles of *PAK7* and previous linkage of this region to JOAG indicate that *PAK7* may have a role in the etiology of glaucoma.

Deletion of 12p33.33 (*TULP3*)

Deletions of *TULP3*, located on 12p33.33, were identified in five individuals (Fig. 2B). TULP3, a member of the tubby-like family of proteins, is thought to bind to the plasma membrane until phosphoinositide hydrolysis occurs, at which point it is released into the nucleus and acts as a transcriptional regulator.[53] Previous expression studies have shown that *TULP3* is active in the ganglion cell layer of the retina.[54] Mutation of other tubby family members such as *tub* and *TULP1* results in retinitis pigmentosa.[55,56] It is worth noting that there is precedence for clinical heterogeneity of genes involved in ocular development. For example, mutations of *PAX6* cause both Aniridia and Peter's anomaly.[57] However, there is no clear role for *TULP3* in any disorder of blindness to date.

Five deletions of *TULP3* were detected in our glaucoma cohort, making them the most frequent CNV of interest identified in this study. The deletion is also novel to DGV and 863 controls from the University of Toronto (Marshall C, personal communication, 2009). Analysis of the genotypes surrounding *TULP3* suggests that four of the five deletion carriers share a haplotype, indicating that an ancestral event may have led to many of these deletions. Of note, the study sample included in this project was subjected to multidimensional scaling as part of a separate GWAS to test for population stratification, with unremarkable results (unpublished data, 2009). Therefore, the increase in *TULP3* CNV frequency in the glaucoma cohort is not likely to be due to population differences between the cohorts.

Duplication and Deletion of 5q23.1

We identified two CNVs (one deletion and one duplication) encompassing the genes *DMXL1* and *DTWD2* on 5q23.1

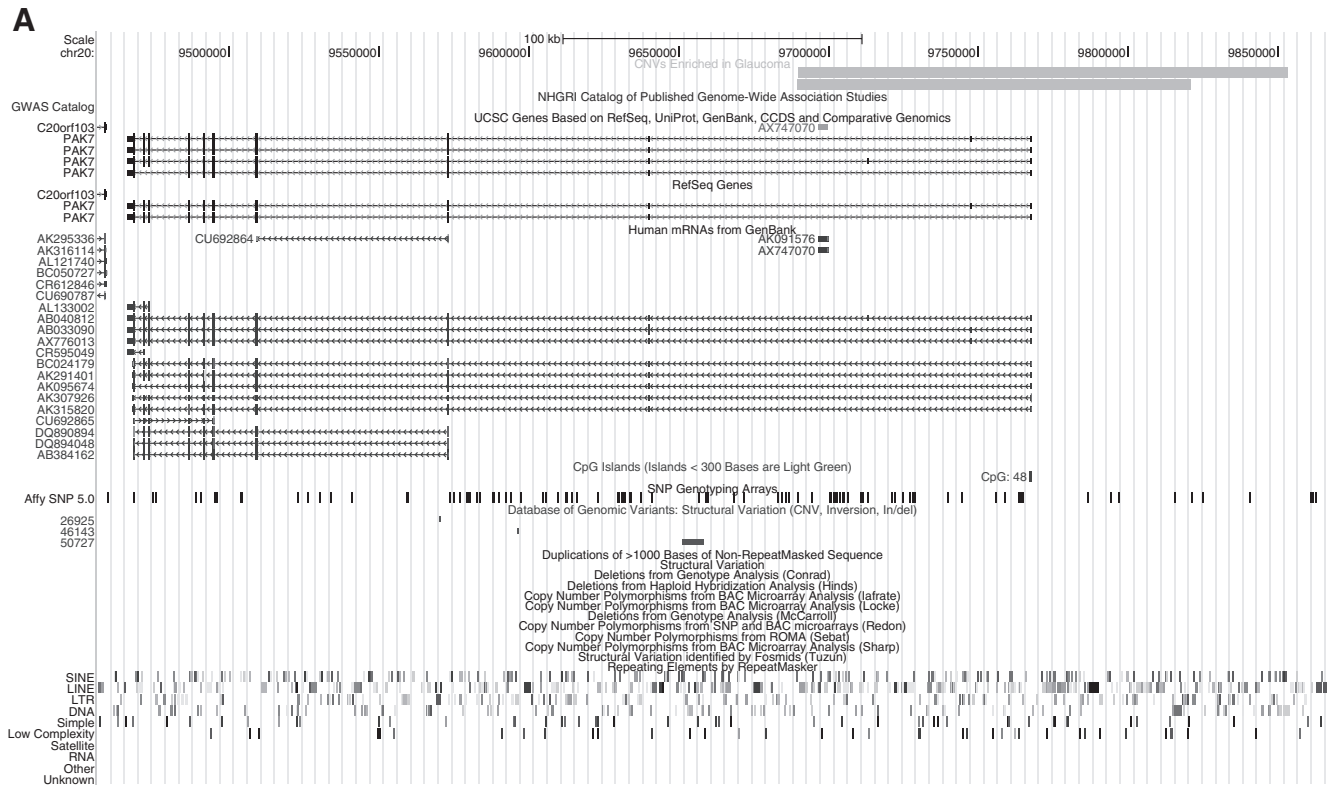

FIGURE 2. UCSC (University of California, Santa Cruz) screen captures representing three CNVs that met criteria for the high-interest group. The tracks displayed in the figures include an NHGRI (National Human Genome Research Institute) catalog of published genome wide association studies, UCSC genes, RefSeq Genes (National Center for Biotechnology Information, Bethesda MD, available at www.ncbi.nlm.nih.gov/locuslink/refseq), human mRNAs from GenBank, CpG islands, SNP density from the 5.0 array (Affymetrix, Santa Clara, CA), DGV structural variation, duplication of nonrepeat masked sequence, structural variation, and repeat elements. (**A**) Duplication of *PAK7* is located on 20p12. The duplications encompass the first two exons of the *PAK7* gene. *Top bar* of the CNVs Enriched in Glaucoma track: the duplication from patient GGA-1079-1 with breakpoints determined by PennCNV at chromosome (chr)20:9,689,876-9,853,180. *Bottom bar*: the duplication identified in patient GGA-410-1 with breakpoints determined by PennCNV at chr20:9689876-9820828.

(Fig. 2C). These CNVs are contained within both the GLC1M linkage locus for JOAG[21,22] and the quantitative traits locus for IOP that was mapped to 5q,[58] and they are near the GLC1G locus for POAG. Small structural variants within *DMXL1* are noted in DGV and have been identified primarily by paired end sequencing in three HapMap controls who were not screened for glaucoma.[25,26,59] However, the CNVs present in our two patients are larger and thus, to our knowledge, novel. They have also not been identified in 862 unpublished controls from the University of Toronto (Marshall C, personal communication, 2009).

Little is known about the function of either *DMXL1* or *DTWD2*. Rotimi et al.,[58] previously identified *DMXL1* as one of many potential glaucoma-causing genes in their 5q locus based on sequence homology with *WDR36*. Interestingly, *DMXL1* is expressed in the retina, the ganglion cell layer, the optic nerve, optic nerve head, iris, lens, and choroid (data from microarray expression study of 10 ocular tissues conducted in collaboration with Alcon; data not shown). The gene contains a WD repeat region that is highly conserved, and, based on sequence similarity to family members, it is predicted to have regulatory function similar to other WD repeat genes.[60] In addition, deletion of *DMXL1* in the context of larger chromosomal abnormalities has been associated with ocular phenotypes including iris coloboma and microphthalmia.[61,62]

Neither of the patients with 5q23.1 CNVs had a history of markedly elevated IOP. Patient GGA-1058-1, who carries the duplication, had no recorded IOP measurements over 21 mm Hg and received a diagnosis of normal-tension glaucoma, whereas patient GGA-1148-1, who carries the deletion, had a maximum IOP of 23 mm Hg. Again, there are no DNA samples available from parents to determine whether these CNVs were inherited or arose de novo, but genotype analysis of the CNV region did not reveal a shared haplotype, and they are unlikely to share a common ancestral event. Patient GGA-1148-1 did have a family history of glaucoma involving two paternal aunts, whereas patient GGA-1058-1 had no family history of glaucoma. Segmental duplications flank *DMXL1* and *DTWD2* suggesting nonallelic homologous recombination as a potential mechanism for these CNVs.

Duplication of 12q14

We also identified a 12q14 duplication (*C12orf56*, *XPOT*, *TBK1*, and *RASSF3*) that was originally detected in an extended normal-tension glaucoma pedigree. The original 12q14 duplication found in that family, the candidate genes it contains, and its relation to the familial phenotype are discussed in depth elsewhere.[63] In this study, we identified two unrelated patients with duplications of 12q14. Both patients (GGA-458-1 and GGA-1159-1) had normal-tension glaucoma. This duplication is also exceedingly rare, and no records of copy number changes in *XPOT* or *TBK1* exist in the DGV. Like other rare variants identified in this study, this CNV was not found in 863 controls from the University of Toronto (Marshall C, personal communication, 2009). Of the genes included in the CNV, *TBK1* is the most likely

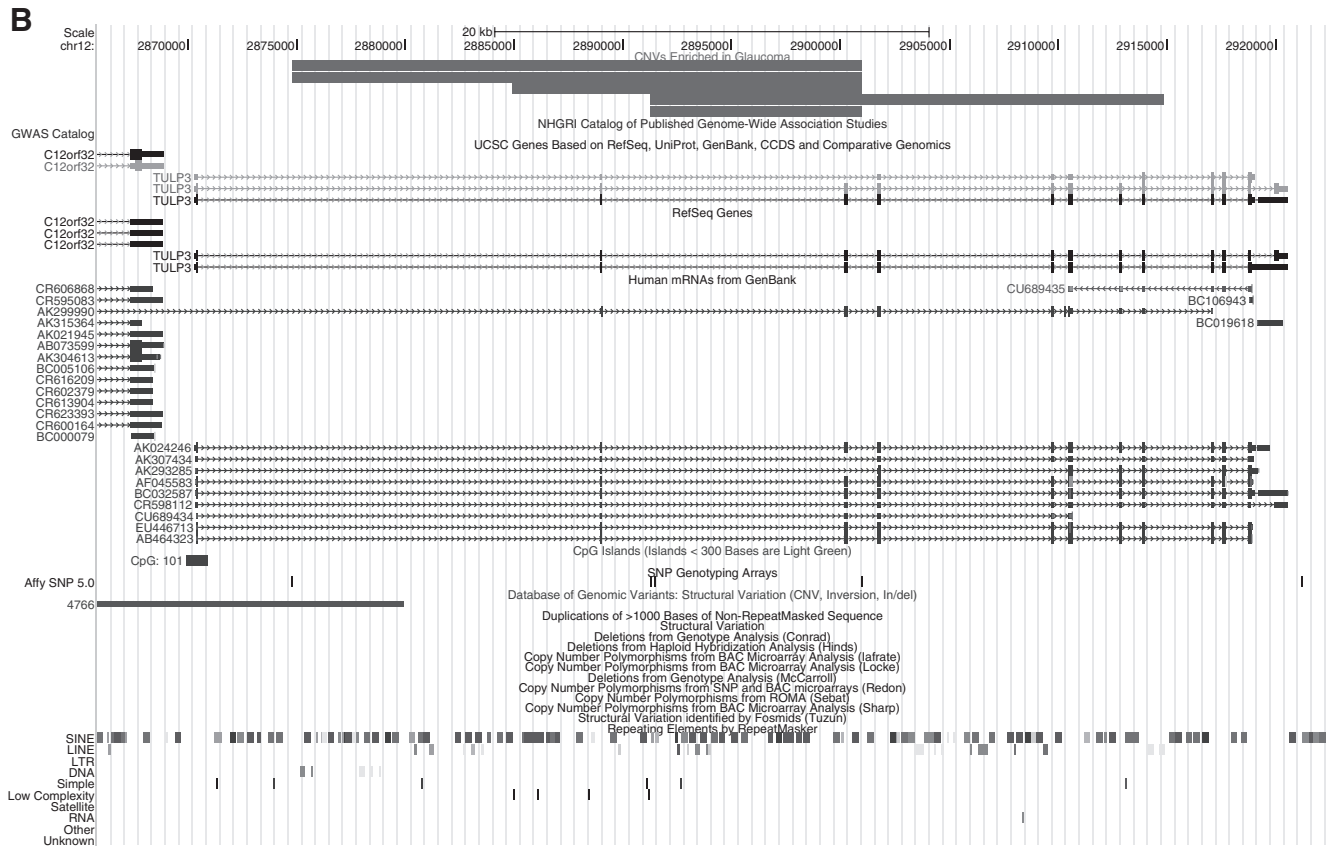

FIGURE 2. (*Continued*) (**B**) Deletions of *TULP3* located on 12p13.33 identified in five patients, in order from top to bottom: GGA-1037-1, GGA-1042-1, GGA-1054-1, GGA-1100-1, and GGA-1108-1. These patients share an overlapping consensus region with breakpoints at chr12: 2,891,255-2,901,000, including exon 3 of *TULP3*.

candidate to play a role in the development of glaucoma. *TBK1* is a serine/threonine protein kinase and has been identified as a binding partner for *OPTN* in a two-hybrid screen. Additional studies indicate that the *OPTN* [E50K] mutant allele associated with retinal ganglion cell loss displays enhanced binding to *TBK1*, suggesting that this interaction plays a role in the POAG caused by the E50K mutation.[64,65]

There are multiple mouse models of *TBK1* mutant alleles; however, the null mutation is embryonically lethal on a C57BL/6 background. A recent paper reported the development of a viable *TBK1* knockout on a 129S5 background and found that the null mice exhibited mononuclear and granulomatous cell infiltrates in several organs including lungs, liver, kidney, spleen, and salivary glands.[66] Unfortunately, the eyes were not described in this study. Based on our findings and previous functional data, *TBK1* appears to be a compelling candidate gene for glaucoma.

Of the remaining genes in the glaucoma CNV set, little is known about their function. Two loci, one on 18p11.32 and one on 5p15.33, contained human ESTs but no RefSeq genes (National Center for Biotechnology Information, Bethesda MD, available at www.ncbi.nlm.nih.gov/locuslink/refseq). Duplications in *CD5* and *CD6*, antigens involved in T-cell regulation, were also identified; duplication of *CD5*, but not *CD6*, has been reported in control samples unscreened for glaucoma.

In addition, we detected single-event CNVs that, while not meeting the criteria for enrichment in glaucoma, are nonetheless of interest. These included a duplication affecting *PAX2*, a deletion affecting *TGFBR3*, and a duplication affecting *WDR36*. *WDR36* is notable because previous reports have suggested that mutations in this gene are associated with glaucoma.[67–69] In addition, there are multiple lines of functional evidence to suggest a mechanism for which WDR36 may play a role in the development of glaucoma.[70–72] However, because *WDR36* duplications were also identified in two of our control individuals, our study does not support a role for CNV of this gene in glaucoma. The *PAX2* duplication subject (GGA-430-1) had a family history of glaucoma that included a maternal grandfather, mother, several aunts, and cousins. This patient with diagnosed glaucoma was noted to have significantly enlarged cup-to-disc ratios (0.9 in the right eye, 0.7 in the left eye) in the fifth decade of life. Mutations of *PAX2* have been associated with retinal and optic nerve colobomas as well as microphthalmia,[73–76] but to our knowledge this is the first report of a *PAX2* structural variant in a patient with POAG.

Conspicuously absent were CNVs in myocilin (*MYOC*) and optineurin (*OPTN*). One explanation for the lack of deletions in MYOC is that haploinsufficiency of *MYOC* does not result in glaucoma.[77] Similarly, it is possible that *OPTN* haploinsufficiency does not produce a phenotype or, alternatively, results in a more severe ocular disorder. However, it is notable that overexpression of *OPTN* through loss of one of the two leucine zipper motifs results in loss of retinal ganglion cells in mice.[64] In addition, we did not identify any CNVs in *FOXC1* or *LMXB1*, probably because these mutations result in congenital forms of glaucoma that are often associated with extraocular manifestations, and such patients would not have been recruited into this study.[37,41,78]

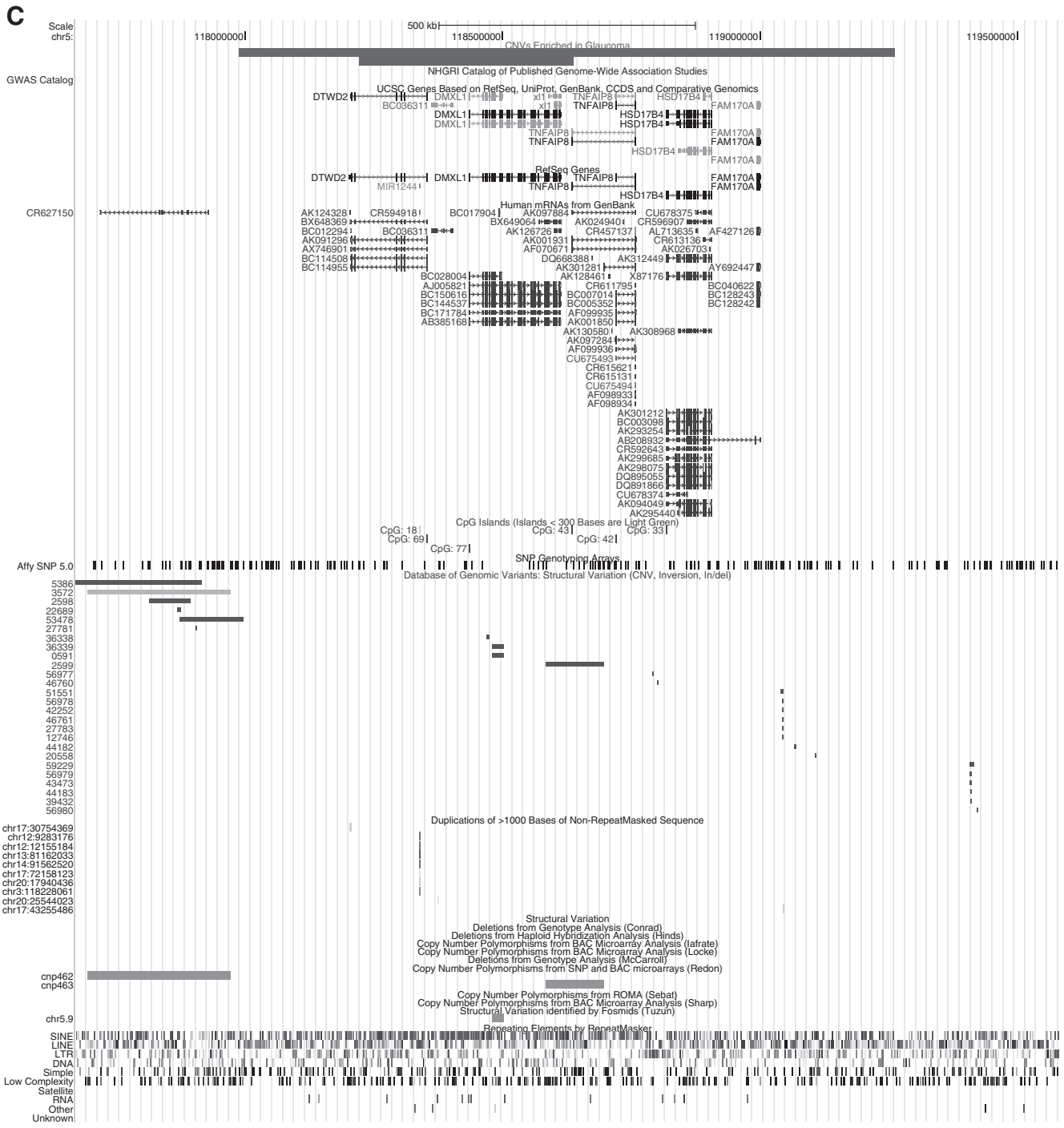

Figure 2. (*Continued*) (**C**) The two patients with CNVs identified on 5p23.1 including the genes *DMXL1* and *DTWD2*. *Top bar* of the CNVs Enriched in Glaucoma track: duplication from patient GGA-1058-1, with breakpoints determined by PennCNV at chr5:117,987,956-119,261,893. *Bottom bar*: deletion identified in patient GGA-1148-1 with breakpoints identified by PennCNV at chr5:118,221,327-118,637,515. The DGV structural variation track shows four CNVs identified in the overlapping consensus region in controls unscreened for glaucoma. *DMXL1*, a member of the WD-repeat family of genes, is an excellent functional candidate in this region, as it is expressed in the retina, ganglion cell layer, optic nerve and optic nerve head, iris, lens, and choroid, according to expression array experiments on 10 ocular tissues conducted in a collaboration between our laboratory and Alcon (Fort Worth, TX; data not shown). *DTWD2*, about which less is known, is an excellent positional candidate, as it is untouched by control CNVs.

Conclusions

We have identified CNVs that implicate several compelling POAG loci and genes that are supported by converging phenotypic data, expression data, and previous linkage data. These data, similar to CNV findings from other disorders, do not generally overlap existing association study findings. This result emphasizes the importance of the CNV approach as a complement to GWAS for detecting pathogenic glaucoma genes and provides an additional set of disease genes that may help to elucidate important molecular pathways that underlie the disorder.

TABLE 5. Phenotype Information Available on Individuals with Genic CNVs of Interest

Patient ID	Genes in CNV	CNV Type	Location	Sex	Age at Diagnosis (y)	Max Recorded IOP (mm Hg)	CCT (μm)	History of Glaucoma Surgery	Family History of Glaucoma
GGA-1079–1	*PAK7*	Dup	20p12	M	59	38 OU	ND	+	–
GGA-410–1	*PAK7*	Dup	20p12	M	63	21OD,25OS	500 OD, 504 OS	+	–
GGA-1148–1	*DMXL1, DTWD2*	Del	5p23.1	F	60	23OD,19OS	587 OD, 596 OS	–	+
GGA-1058–1	*DMXL1, DTWD2*	Dup	5p23.1	F	47	19OD,20OS	493 OD, 468 OS	+	–
GGA-1100–1	*TULP3*	Del	12p13.33	M	46	34OD,24OS	506 OD, 493 OS	+	+
GGA-1109–1	*TULP3*	Del	12p13.33	F	70	21OD,24OS	511 OD, 497 OS	+	+
GGA-1042–1	*TULP3*	Del	12p13.33	M	70	30OD,20OS	549 OD, 536 OS	+	+
GGA-1054–1	*TULP3*	Del	12p13.33	M	63	46OD,20OS	527 OD, 534 OS	+	–
GGA-1037–1	*TULP3*	Del	12p13.33	M	69	19OD,24OS	536 OD, 524 OS	–	+
GGA-430–1	*PAX2*	Dup	10q24.31	F	42	23OD,20OS	550 OD, 537 OS	+	+
GGA-215–1	*TGFBR3*	Del	1p22.2-p22.1	F	ND	ND	ND	+	ND
GGA-458–1	*C12orf56, XPOT, XPOT, TBK1, RASSF3*	Dup	12q14.2	M	33	17 OU	ND	+	+
GGA-1159–1	*C12orf56, XPOT, TBK1, RASSF3*	Dup	12q14.2	F	58	20 OU	549 OD, 571 OS	+	–

Genes included in the CNV region and the type of CNV are listed for each individual. Clinical variables including sex, age at diagnosis, maximum recorded IOP and CCT are reported along with history of glaucoma surgery and family history of disease. Del, deletion; dup, duplication; ND, no data available.

One limitation of our study is that, as with any age-related disorder, it is impossible to ensure that none of the AMD subjects will eventually develop glaucoma. However, the control set is used as a screening tool to filter out common and benign rare CNV results from the POAG data. Therefore the possibility of there being glaucoma-positive patients within the control set would have the effect of making our analysis overly conservative and of increasing type II errors, but is unlikely to contribute to false-positive results.

An additional limitation of our study is that a majority of the control patients are not true controls but are instead disease contrast patients. Our study, which was intended to indentify rare variants involved in glaucoma hinges primarily on contrasting two sets of individuals, with one set highly enriched for glaucoma and the other set glaucoma-depleted. Therefore, an alternative explanation for the data does exist, which is that these rare CNVs may be protective against AMD. This secondary explanation is not incompatible with the most parsimonious explanation of the data, which is that the rare CNVs found in the POAG sample increase susceptibility to glaucoma.

Based on some of the converging factors highlighted in this study including (1) the presence of these rare events in the glaucoma population and the paucity of these events in our nonglaucoma case/contrast sample and in unselected control databases (DGV), (2) the overlap of linkage signals and CNV locations, (3) the expression patterns of the genes affected by the CNVs in question, and (4) the phenotypes of patients who share CNVs, we believe that these variants should each be considered candidates for further study in glaucoma. Replication studies in much larger samples and functional studies in model systems are necessary, to confirm a role for these rare variants in the pathophysiology of glaucoma.

Acknowledgments

The authors thank the patients and their families for participating in the study; and Christian Marshall and Kai Wang for helpful discussions regarding data analysis.

References

1. Sommer A, Tielsch JM, Katz J, et al. Relationship between intraocular pressure and primary open angle glaucoma among white and black Americans. The Baltimore Eye Survey. *Arch Ophthalmol.* 1991;109:1090–1095.
2. Gordon MO, Beiser JA, Brandt JD, et al. The Ocular Hypertension Treatment Study: baseline factors that predict the onset of primary open-angle glaucoma. *Arch Ophthalmol.* 120:714–720, 2002; discussion 829–730.
3. Kwon YH, Fingert JH, Kuehn MH, Alward WLM. Mechanism of disease: Primary Open Angle Glaucoma. *N Engl J Med.* 2009; 360(11):1113–1124.
4. Klein R, Klein BE, Tomany SC, Wong TY. The relation of retinal microvascular characteristics to age-related eye disease: the Beaver Dam eye study. *Am J Ophthalmol.* 2004;137:435–444.
5. Sheffield VC, Stone EM, Alward WL, et al. Genetic linkage of familial open angle glaucoma to chromosome 1q21–q31. *Nat Genet.* 1993;4:47–50.
6. Stone EM, Fingert JH, Alward WL, et al. Identification of a gene that causes primary open angle glaucoma. *Science.* 1997;275:668–670.
7. Stoilova D, Child A, Trifan O, Crick RP, Coakes RL, Sarfarazi M. Localization of a locus (GLC1B) for adult-onset primary open angle glaucoma to the 2cen-q13 region. *Genomics.* 1996;36:142–150.
8. Wirtz MK, Samples JR, Kramer PL, et al. Mapping a gene for adult-onset primary open-angle glaucoma to chromosome 3q. *Am J Hum Genet.* 1997;60:296–304.
9. Kitsos G, Eiberg H, Economou-Petersen E, et al. Genetic linkage of autosomal dominant primary open angle glaucoma to chromo-

some 3q in a Greek pedigree. *Europ J Hum Genet.* 2001;9:452–457.

10. Trifan OC, Traboulsi El, Stoilova D, et al. A third locus (GLC1D) for adult-onset primary open-angle glaucoma maps to the 8q23 region. *Am J Ophthal.* 1998;126:17–28.
11. Rezaie T, Child A, Hitchings R, et al. Adult-onset primary open-angle glaucoma caused by mutations in optineurin. *Science.* 2002; 295:1077–1079.
12. Sarfarazi M, Child A, Stoilova D, et al. Localization of the fourth locus (GLC1E) for adult-onset primary open-angle glaucoma to the 10p15–p14 region. *Am J Hum Genet.* 1998;62:641–652.
13. Wirtz MK, Samples JR, Rust K, et al. GLC1F, a new primary open-angle glaucoma locus, maps to 7q35-q36. *Arch Ophthal.* 1999;117:237–241.
14. Monemi S, Spaeth G, DaSilva A, et al. Identification of a novel adult-onset primary open-angle glaucoma (POAG) gene on 5q22.1. *Hum Mol Genet.* 2005;14:725–733.
15. Suriyapperuma SP, Child A, Desai T, et al. A new locus (GLC1H) for adult-onset primary open-angle glaucoma maps to the 2p15-p16 region. *Arch Ophthal.* 2007;125:86–92.
16. Wiggs JL, Allingham RR, Hossain A, et al. Genome-wide scan for adult onset primary open angle glaucoma. *Hum Molec Genet.* 2000;9:1109–1117.
17. Allingham RR, Wiggs JL, Hauser ER, et al. Early adult-onset POAG linked to 15q11-13 using ordered subset analysis. *Invest Ophthal Vis Sci.* 2005;46:2002–2005.
18. Wiggs JL, Lynch S, Ynagi G, et al. A genomewide scan identifies novel early-onset primary open-angle glaucoma loci on 9q22 and 20p12. *Am J Hum Genet.* 2004;74:1314–1320.
19. Sud A, Del Bono EA, Haines JL, Wiggs JL. Fine mapping of the GLC1K juvenile primary open-angle glaucoma locus and exclusion of candidate genes. *Mol Vis.* 2008;14:1319–1326.
20. Baird PN, Foote SJ, Mackey DA, Craig J, Speed TP, Bureau A. Evidence for a novel glaucoma locus at chromosome 3p2l-22. *Hum Genet.* 2005;117:249–257.
21. Pang CP, Fan BJ, Canlas O, et al. A genome-wide scan maps a novel juvenile-onset primary open angle glaucoma locus to chromosome 5q. *Mol Vis.* 2006;12:85–92.
22. Fan BJ, Ko WC, Wang DY, et al. Fine mapping of new glaucoma locus GLC1M and exclusion of neuregulin 2 as the causative gene. *Mol Vis.* 2007;13:779–784.
23. Wang DY, Fan BJ, Chua JKH, et al. A genome-wide scan maps a novel juvenile-onset primary open-angle glaucoma locus to 15q. *Invest Ophthal Vis Sci.* 2006,47:5315–5321.
24. Fingert JH, Stone EM, Sheffield VC, Alward WL. Myocilin glaucoma. *Surv Ophthalmol.* 2002;47:547–561.
25. Redon R, Ishikawa S, Fitch KR, et al. Global variation in copy number in the human genome. *Nature.* 2006;444:444–454.
26. Kidd JM, Cooper GM, Donahue WF, et al. Mapping and sequencing of structural variation from eight human genomes. *Nature.* 2008; 453:56–64.
27. Itsara A, Cooper GM, Baker C, et al. Population analysis of large copy number variants and hotspots of human genetic disease. *Am J Hum Genet.* 2009;84:148–161.
28. Pinto D, Marshall C, Feuk L, Scherer SW. Copy-number variation in control population cohorts. *Hum Mol Genet*. 2007;16(Spec. No. 2):R168–R173.
29. Bassett AS, Marshall CR, Lionel AC, Chow EW, Scherer SW. Copy number variations and risk for schizophrenia in 22q11.2 deletion syndrome. *Hum Mol Genet.* 2008;17:4045–4053.
30. Marshall CR, Noor A, Vincent JB, et al. Structural variation of chromosomes in autism spectrum disorder. *Am J Hum Genet.* 2008;82:477–488.
31. Xu B, Roos JL, Levy S, van Rensburg EJ, Gogos JA, Karayiorgou M. Strong association of de novo copy number mutations with sporadic schizophrenia. *Nat Genet.* 2008;40:880–885.
32. Glessner JT, Wang K, Cai G, et al. Autism genome-wide copy number variation reveals ubiquitin and neuronal genes. *Nature.* 2009;459:569–573.
33. Fellermann K, Stange DE, Schaeffeler E, et al. A chromosome 8 gene-cluster polymorphism with low human beta-defensin 2 gene copy number predisposes to Crohn disease of the colon. *Am J Hum Genet.* 2006;79:439–448.
34 Sebat J, Lakshmi B, Troge J, et al. Large-scale copy number polymorphism in the human genome. *Science.* 2004;305:525–528.
35. Bongers EM, de Wijs IJ, Marcelis C, Hoefsloot LH, Knoers NV. Identification of entire LMX1B gene deletions in nail patella syndrome: evidence for haploinsufficiency as the main pathogenic mechanism underlying dominant inheritance in man. *Eur J Hum Genet.* 2008;16:1240–1244.
36. Connell P, Brosnahan D, Dunlop A, Reardon W. Bilateral optic disk swelling in the 4q34 deletion syndrome. *J AAPOS.* 2007;11:516–518.
37. Nishimura DY, Swiderski RE, Alward WL, et al. The forkhead transcription factor gene FKHL7 is responsible for glaucoma phenotypes which map to 6p25. *Nat Genet.* 1998;19:140–147.
38. Rouillac C, Roche O, Marchant D, et al. Mapping of a congenital microcoria locus to 13q31–q32. *Am J Hum Genet.* 1998;62:1117–1122.
39. Cohn AC, Kearns LS, Savarirayan R, Ryan J, Craig JE, Mackey DA. Chromosomal abnormalities and glaucoma: a case of congenital glaucoma with trisomy 8q22-qter/ monosomy 9p23-pter. *Ophthalmic Genet.* 2005;26:45–53.
40. Sakata R, Usui T, Mimaki M, Araie M. Developmental glaucoma with chromosomal abnormalities of 9p deletion and 13q duplication. *Arch Ophthalmol.* 2008;126:431–432.
41. Nishimura DY, Searby CC, Alward WL, et al. A spectrum of FOXC1 mutations suggests gene dosage as a mechanism for developmental defects of the anterior chamber of the eye. *Am J Hum Genet.* 2001;68:364–372.
42. Chanda B, Asai-Coakwell M, Ye M, et al. A novel mechanistic spectrum underlies glaucoma-associated chromosome 6p25 copy number variation. *Hum Mol Genet.* 2008;17:3446–3458.
43. Abu-Amero KK, Hellani A, Bender P, et al. High-resolution analysis of DNA copy number alterations in patients with primary open-angle glaucoma. *Mol Vis.* 2009;15:1594–1598.
44. Gordon MO, Kass MA. The Ocular Hypertension Treatment Study: design and baseline description of the participants. *Arch Ophthalmol.* 1999;117:573–583.
45. Collaborative Normal Tension Glaucoma Study Group (CNTGS). The effectiveness of intraocular pressure reduction in the treatment of normal-tension glaucoma. *Am J Ophthalmol.* 1998;126(4): 496–505.
46. Wang K, Li M, Hadley D, et al. PennCNV: an integrated hidden Markov model designed for high-resolution copy number variation detection in whole-genome SNP genotyping data. *Genome Res.* 2007;17:1665–1674.
47. Nannya Y, Sanada M, Nakazaki K, et al. A robust algorithm for copy number detection using high-density oligonucleotide single nucleotide polymorphism genotyping arrays. *Cancer Res.* 2005;65: 6071–6079.
48. Li C, Wong WH. Model-based analysis of oligonucleotide arrays: expression index computation and outlier detection. *Proc Natl Acad Sci U S A.* 2001;98:31–36.
49. Lin M, Wei LJ, Sellers WR, Lieberfarb M, Wong WH, Li C. dChipSNP: significance curve and clustering of SNP-array-based loss-of-heterozygosity data. *Bioinformatics.* 2004;20:1233–1240.
50. Diskin SJ, Li M, Hou C, et al. Adjustment of genomic waves in signal intensities from whole-genome SNP genotyping platforms. *Nucleic Acids Res.* 2008;36:e126.
51. Li X, Minden A. Targeted disruption of the gene for the PAK5 kinase in mice. *Mol Cell Biol.* 2003;23:7134–7142.
52. Matenia D, Griesshaber B, Li XY, et al. PAK5 kinase is an inhibitor of MARK/Par-1, which leads to stable microtubules and dynamic actin. *Mol Biol Cell.* 2005;16:4410–4422.
53. Santagata S, Boggon TJ, Baird CL, et al. G-protein signaling through tubby proteins. *Science.* 2001;292:2041–2050.
54. Ikeda S, He W, Ikeda A, Naggert JK, North MA, Nishina PM. Cell-specific expression of tubby gene family members (tub, Tulp1,2, and 3) in the retina. *Invest Ophthalmol Vis Sci.* 1999;40: 2706–2712.
55. Hagstrom SA, North MA, Nishina PL, Berson EL, Dryja TP. Recessive mutations in the gene encoding the tubby-like protein TULP1 in patients with retinitis pigmentosa. *Nat Genet.* 1998;18:174–176.

56. Banerjee P, Kleyn PW, Knowles JA, et al. TULP1 mutation in two extended Dominican kindreds with autosomal recessive retinitis pigmentosa. *Nat Genet.* 1998;18:177–179.
57. Hanson IM, Fletcher JM, Jordan T, et al. Mutations at the PAX6 locus are found in heterogeneous anterior segment malformations including Peters' anomaly. *Nat Genet.* 1994;6:168–173.
58. Rotimi CN, Chen G, Adeyemo AA, et al. Genomewide scan and fine mapping of quantitative trait loci for intraocular pressure on 5q and 14q in West Africans. *Invest Ophthalmol Vis Sci.* 2006;47: 3262–3267.
59. Tuzun E, Sharp AJ, Bailey JA, et al. Fine-scale structural variation of the human genome. *Nat Genet.* 2005;37:727–732.
60. Kraemer C, Enklaar T, Zabel B, Schmidt ER. Mapping and structure of DMXL1, a human homologue of the DmX gene from Drosophila melanogaster coding for a WD repeat protein. *Genomics.* 2000; 64:97–101.
61. Yung JF, Williamson N, Salafsky I, Hoo JJ. Deletion of band 5q21 in association with a de novo translocation involving 2p and 5q. *J Med Genet.* 1988;25:570–572.
62. Garcia-Minaur S, Ramsay J, Grace E, Minns RA, Myles LM, FitzPatrick DR. Interstitial deletion of the long arm of chromosome 5 in a boy with multiple congenital anomalies and mental retardation: molecular characterization of the deleted region to 5q22.3q23.3. *Am J Med Genet A.* 2005;132:402–410.
63. Fingert JH, Robin AL, Stone JL, et al. Copy number variations on chromosome 12q14 in patients with normal tension glaucoma. *Hum Mol Genet.* 2011;15:20(12):2482–2494.
64. Morton S, Hesson L, Peggie M, Cohen P. Enhanced binding of TBK1 by an optineurin mutant that causes a familial form of primary open angle glaucoma. *FEBS Lett.* 2008;582:997–1002.
65. Chi ZL, Akahori M, Obazawa M, et al. Overexpression of optineurin E50K disrupts Rab8 interaction and leads to a progressive retinal degeneration in mice. *Hum Mol Genet.* 2010;19:2606–2615.
66. Marchlik E, Thakker P, Carlson T, et al. Mice lacking Tbk1 activity exhibit immune cell infiltrates in multiple tissues and increased susceptibility to LPS-induced lethality. *J Leukoc Biol.* 2010;88: 1171–1180.
67. Hewitt AW, Dimasi DP, Mackey DA, Craig JE. A glaucoma case-control study of the WDR36 gene D658G sequence variant. *Am J Ophthalmol.* 2006;142:324–325.
68. Hauser MA, Allingham RR, Linkroum K, et al. Distribution of WDR36 DNA sequence variants in patients with primary open-angle glaucoma. *Invest Ophthalmol Vis Sci.* 2006;47:2542–2546.
69. Fingert JH, Alward WL, Kwon YH, et al. No association between variations in the WDR36 gene and primary open-angle glaucoma. *Arch Ophthalmol.* 2007;125:434–436.
70. Skarie JM, Link BA. The primary open-angle glaucoma gene WDR36 functions in ribosomal RNA processing and interacts with the p53 stress-response pathway. *Hum Mol Genet.* 2008;17:2474–2485.
71. Footz TK, Johnson JL, Dubois S, Boivin N, Raymond V, Walter MA. Glaucoma-associated WDR36 variants encode functional defects in a yeast model system. *Hum Mol Genet.* 2009;18:1276–1287.
72. Chi ZL, Yasumoto F, Sergeev Y, et al. Mutant WDR36 directly affects axon growth of retinal ganglion cells leading to progressive retinal degeneration in mice. *Hum Mol Genet.* 2010;19:3806–3815.
73 Sanyanusin P, McNoe LA, Sullivan MJ, Weaver RG, Eccles MR. Mutation of PAX2 in two siblings with renal-coloboma syndrome. *Hum Mol Genet.* 1995;4:2183–2184.
74. Schimmenti LA, Shim HH, Wirtschafter JD, et al. Homonucleotide expansion and contraction mutations of PAX2 and inclusion of Chiari 1 malformation as part of renal-coloboma syndrome. *Hum Mutat.* 1999;14:369–376.
75. Tellier AL, Amiel J, Delezoide AL, et al. Expression of the PAX2 gene in human embryos and exclusion in the CHARGE syndrome. *Am J Med Genet.* 2000;93:85–88.
76. Amiel J, Audollent S, Joly D, et al. PAX2 mutations in renal-coloboma syndrome: mutational hotspot and germline mosaicism. *Eur J Hum Genet.* 2000;8:820–826.
77. Shepard AR, Jacobson N, Millar JC, et al. Glaucoma-causing myocilin mutants require the peroxisomal targeting signal-1 receptor (PTS1R) to elevate intraocular pressure. *Hum Mol Genet.* 2007; 16:609–617.
78. Maclean K, Smith J, St Heaps L, et al. Axenfeld-Rieger malformation and distinctive facial features: clues to a recognizable 6p25 microdeletion syndrome. *Am J Med Genet A.* 2005;132:381–385.